

Electronic Supplementary Information (ESI)

Photoswitches with Different Numbers of Azo Chromophores for Molecular Solar Thermal Storage

Shaodong Sun,^a Shuofeng Liang,^a Wen-Cong Xu,^a Minghao Wang,^a Jiangang Gao,^b
Qijin Zhang*^a and Si Wu*^a

^aCAS Key Laboratory of Soft Matter Chemistry, Anhui Key Laboratory of Optoelectronic Science and Technology, Department of Polymer Science and Engineering, University of Science and Technology of China, Hefei 230026, China

E-mail: zqjm@ustc.edu.cn; siwu@ustc.edu.cn

^bSchool of Chemical and Environmental Engineering, Anhui Polytechnic University, Wuhu 241000, China

1. Materials

4-Methoxyazobenzene (**1**, 99%) was purchased from Aladdin Chemical Reagent, Shanghai. Toluene (99.5%), phenol (99%), sodium nitrite (NaNO_2 , 99%), hydrochloric acid (HCl , 36.0~38.0%), acetone (AR), sodium hydroxide (NaOH , 96%), potassium carbonate (K_2CO_3 , 99%), methanol (AR), sodium sulfate (Na_2SO_4 , 99.5%), and sodium chloride (NaCl , 99.5%) were purchased from Sinopharm Chemical Reagent, Shanghai. Petroleum ether (PE, AR), ethyl acetate (EA, AR), and dichloromethane (DCM, AR) were purchased from CHRON CHEMICALS, Chengdu. 3'-Aminoacetanilide (98%) was purchased from 3AChem. Urea (99%) was purchased from Macklin Chemical Reagent, Shanghai. Iodomethane (99.5%), 4-iodoanisole (98%), tert-butyl carbazate (98%), caesium carbonate (Cs_2CO_3 , 99.9%), dimethyl sulfoxide (DMSO, Extra Dry), palladium acetate ($\text{Pd}(\text{OAc})_2$, 99%), 1,3,5-tribromobenzene (99%), and N,N-dimethylformamide (DMF, Extra Dry) were purchased from Energy Chemical Co. Ltd. Copper(I) iodide (CuI , 99%) and tri-tert-butylphosphine (10% in n-pentane) were purchased from Adamas Reagent Co., Ltd.

Toluene was pre-dried over activated 4 Å molecular sieves and heated to reflux over calcium hydride (CaH_2) for 24 h under nitrogen atmosphere and collected by distillation. All other reagents were used without further purification.

2. Instruments and Characterization

The ^1H NMR and ^{13}C NMR analyses were performed on a Bruker Avance III 400MHz NMR spectrometer using CDCl_3 or DMSO-d_6 as the solvent. Chemical shifts are reported in δ units relative to CDCl_3 or DMSO-d_6 [TMS, ^1H δ = 0; CDCl_3 , ^1H δ = 7.26, ^{13}C δ = 77.16; DMSO-d_6 , ^1H δ = 2.50]. The UV-vis absorption spectra were measured on a Shimadzu UV-2600 spectrometer. During the UV-vis absorption tests, the solution was sealed in a quartz cuvette with a knob to prevent solvent volatilization. Optical microscopy (OM) images and polarized optical microscopy (POM) images were captured using an Olympus microscope equipped with a charge-coupled device (CCD) camera. The photoisomerization of azobenzene chromophores was induced with light-

emitting diodes (LEDs) with wavelengths of 365 and 530 nm (Mightex Systems, device types LCS-0365-07-22 and LCS-0530-15-22). The intensity of the UV light (~365 nm) was approximately 3.4 mW/cm². The intensity of the visible light (~530 nm) was approximately 7.6 mW/cm². A solar lamp (Philips full spectrum LED lamp, 22.2 mW/cm²) was used to simulate sunlight. The light intensity was measured using a laser power meter (Model LP100, Changchun New Industries Optoelectronics Technology Co., Ltd.) by exposing the probe vertically under the light source at a specific place. Thermogravimetric analysis (TGA) measurements were conducted on a Shimadzu DTG-60H system with a heating rate of 10 °C/min under a N₂ atmosphere. Differential scanning calorimetry (DSC) data were collected using a Mettler Toledo DSC-3 system under a N₂ atmosphere with a heating or cooling rate of 10 °C/min. High resolution mass spectrometry (HR MS) were recorded by the mass spectrometry service at University of Science and Technology of China (C1-35, Br-79). X-ray diffraction (XRD) patterns were measured on a Multifunctional Rotating-anode X-ray Diffractometer (Instrument model: SmartLab).

3. Synthesis of 2

The synthesis of **2** was based on the method reported in the literature with minor modifications (Figure S1).¹ The details for the synthesis are provided below.

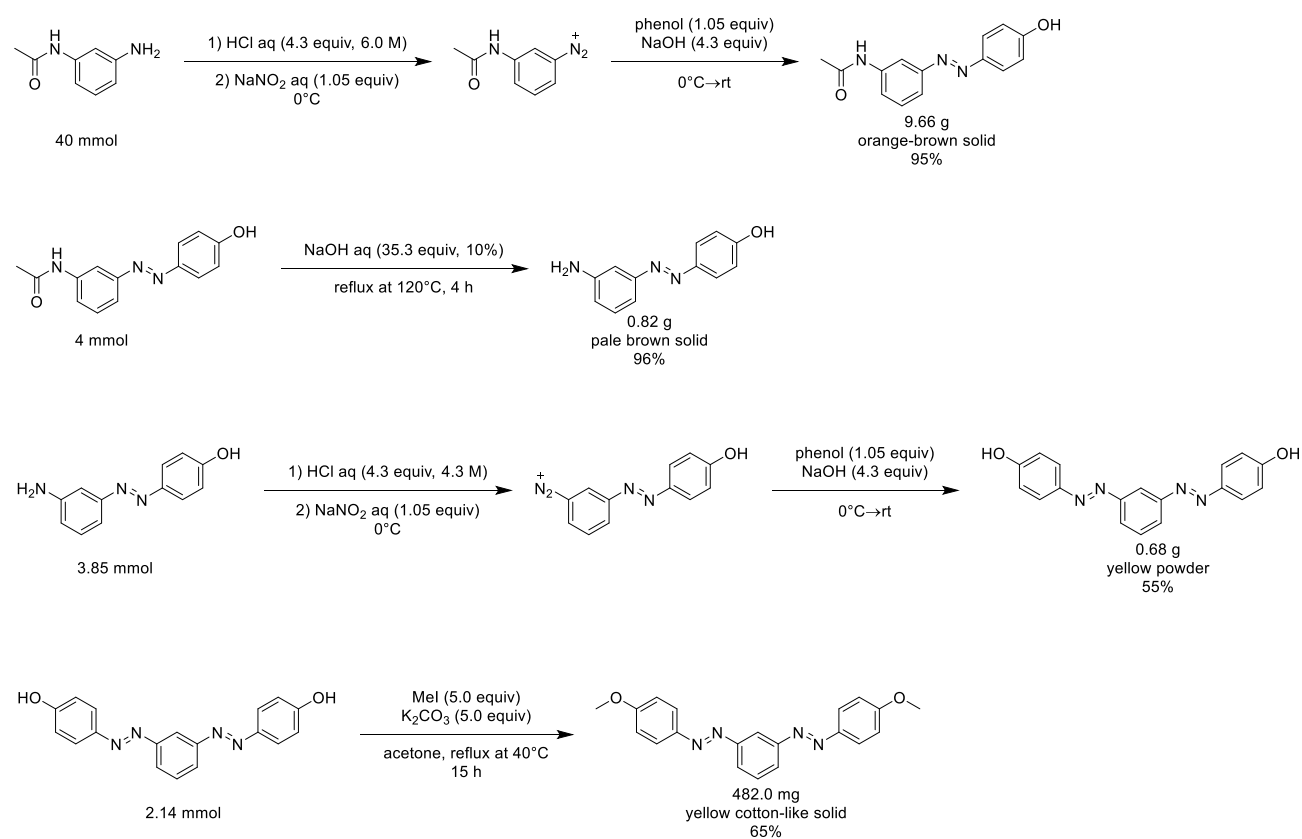
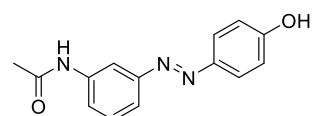


Figure S1. Synthetic route towards **2**.



(E)-N-(3-((4-hydroxyphenyl)diazenyl)phenyl)acetamide: 3'-Aminoacetanilide (6.00 g, 40 mmol, 1.0 equiv) was dissolved in a mixture of HCl (6 mol L⁻¹, 28.7 mL, 172 mmol, 4.3 equiv), ice (20 g), and acetone (20 mL). The mixture was cooled to 0 °C and diazotised by adding a cold solution containing water (20 mL), ice (10 g), and NaNO₂ (2.90 g, 42 mmol, 1.05 equiv) slowly to keep the temperature of the reaction mixture below 5 °C. Then, a cold solution containing phenol (3.95 g, 42 mmol, 1.05 equiv), NaOH (6.88 g, 172 mmol, 4.3 equiv), water (10 mL), and ice (10 g) was added to the mixture slowly. The reaction mixture was stirred for 5 h at pH 9 to 10. The slurry was carefully acidified with HCl (1 mol L⁻¹) to about pH 6. Filtration of the resulting mixture, washing with water, and drying in an oven under vacuum afforded (*E*)-N-(3-((4-hydroxyphenyl)diazenyl)phenyl)acetamide as an orange-brown solid (9.66 g, 95% yield). ¹H NMR (400 MHz, DMSO-d₆) δ 10.33 (s, 1 H), 10.18 (s, 1 H), 8.09 (t, *J* = 1.6

Hz, 1 H), 7.81-7.77 (m, 2 H), 7.67 (dt, $J = 7.6$ Hz, $J = 1.6$ Hz, 1 H), 7.52-7.44 (m, 2 H), 6.96-6.93 (m, 2 H), 2.08 (s, 3 H).

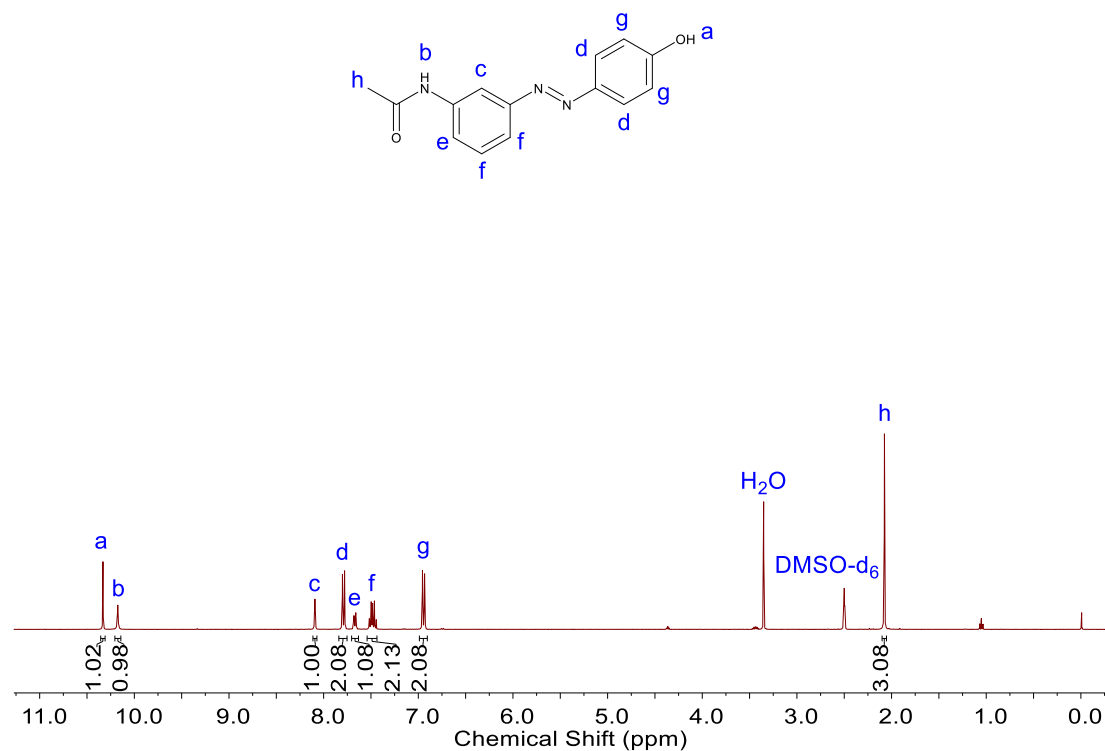
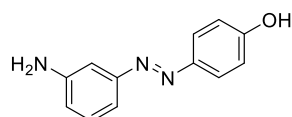


Figure S2. ^1H NMR spectrum of (*E*)-*N*-(3-((4-hydroxyphenyl)diazenyl)phenyl)acetamide.



(*E*)-4-((3-aminophenyl)diazenyl)phenol:

(*E*)-*N*-(3-((4-hydroxyphenyl)diazenyl)phenyl)acetamide (1.02 g, 4 mmol, 1.0 equiv) was dissolved in 10% NaOH aqueous solution (51 mL, 141.2 mmol, 35.3 equiv). The reaction mixture was refluxed at 120 °C for 4 h. The reaction was monitored by thin-layer chromatography (TLC). After completion of the reaction, the mixture was then cooled to room temperature and the pH was adjusted to 6 with conc. HCl. The resulting precipitate was filtered, washed with water and dried in vacuo, affording (*E*)-4-((3-aminophenyl)diazenyl)phenol as a pale brown solid (0.82 g, 96% yield). The compound was sufficiently pure to be used in the subsequent step without any further purification. ^1H NMR (400 MHz, DMSO- d_6) δ 10.24 (s, 1 H), 7.76-7.72 (m, 2 H), 7.20-7.16 (m, 1

H), 7.01-7.00 (m, 2 H), 6.94-6.90 (m, 2 H), 6.68 (ddd, $J = 8.0$ Hz, $J = 2.4$ Hz, $J = 1.2$ Hz, 1 H), 5.36 (s, 2 H).

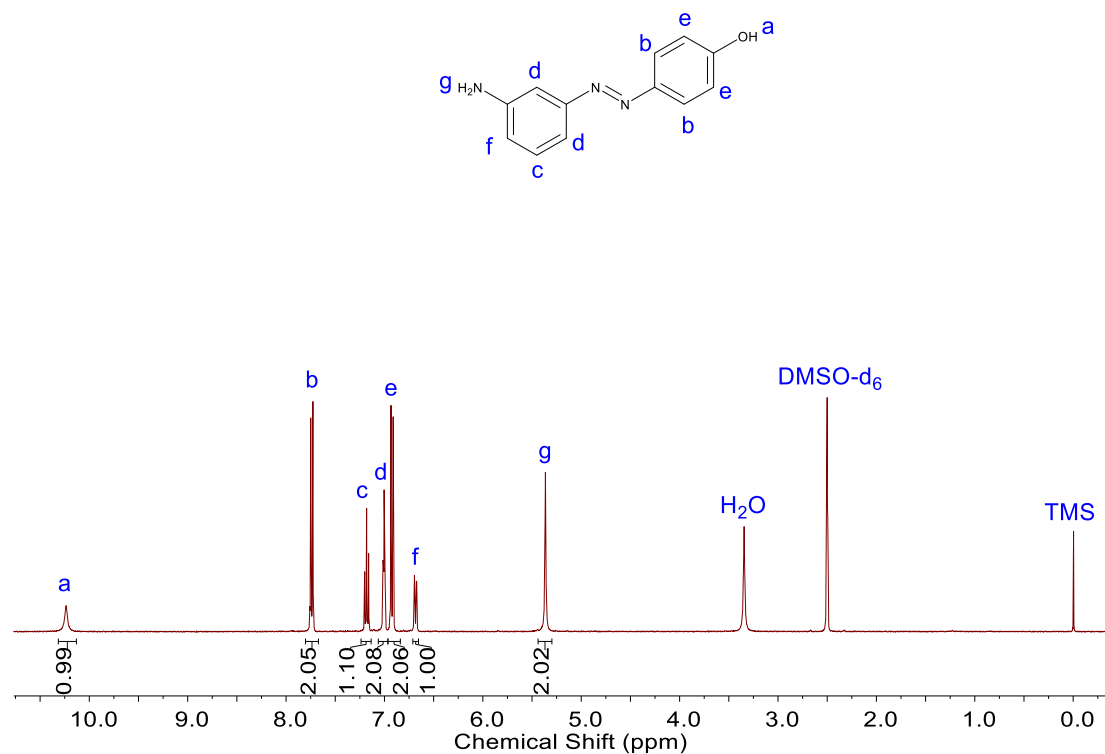
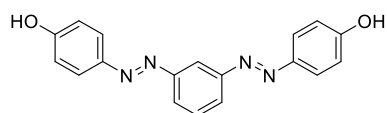


Figure S3. ^1H NMR spectrum of (*E*)-4-((3-aminophenyl)diazenyl)phenol.



4,4'-((1*E*,1'*E*)-1,3-phenylenebis(diazeno-2,1-diyl))diphenol:

(*E*)-4-((3-aminophenyl)diazenyl)phenol (0.82 g, 3.85 mmol, 1.0 equiv) was dissolved in a mixture of HCl (4.3 mol L⁻¹, 3.9 mL, 16.56 mmol, 4.3 equiv), ice (20 g), and acetone (12 mL). The mixture was cooled to 0 °C and diazotised by adding a cold solution containing water (5 mL), ice (5 g), and NaNO₂ (278.8 mg, 4.04 mmol, 1.05 equiv) slowly to keep the temperature of the reaction mixture below 5 °C. When the addition was finished, iodine-starch paper gave a positive test, indicating that the diazotization was successfully completed. A few crystals of urea were added. Then, a cold solution containing phenol (380.2 mg, 4.04 mmol, 1.05 equiv), NaOH (0.66 g, 16.56 mmol, 4.3 equiv), water (3 mL), and ice (2 g) was added to the mixture slowly.

The reaction mixture was stirred for 5 h at pH 9 to 10. The slurry was carefully acidified with HCl (1 mol L⁻¹) to about pH 6. Filtration of the resulting mixture, washing with water, and drying in an oven under vacuum afforded yellow crude product. The crude product was purified by column chromatography over silica gel (petroleum ether/ethyl acetate = 5/2 as the eluent), giving 4,4'-((1*E*,1'*E*)-1,3-phenylenebis(diazene-2,1-diyl))diphenol as yellow powders (0.68 g, 55% yield). ¹H NMR (400 MHz, DMSO-d₆) δ 10.42 (s, 2 H), 8.16 (t, *J* = 1.6 Hz, 1 H), 7.96 (dd, *J* = 7.6 Hz, *J* = 2.0 Hz, 2 H), 7.88-7.85 (m, 4 H), 7.74 (t, *J* = 7.6 Hz, 1 H), 6.99-6.95 (m, 4 H).

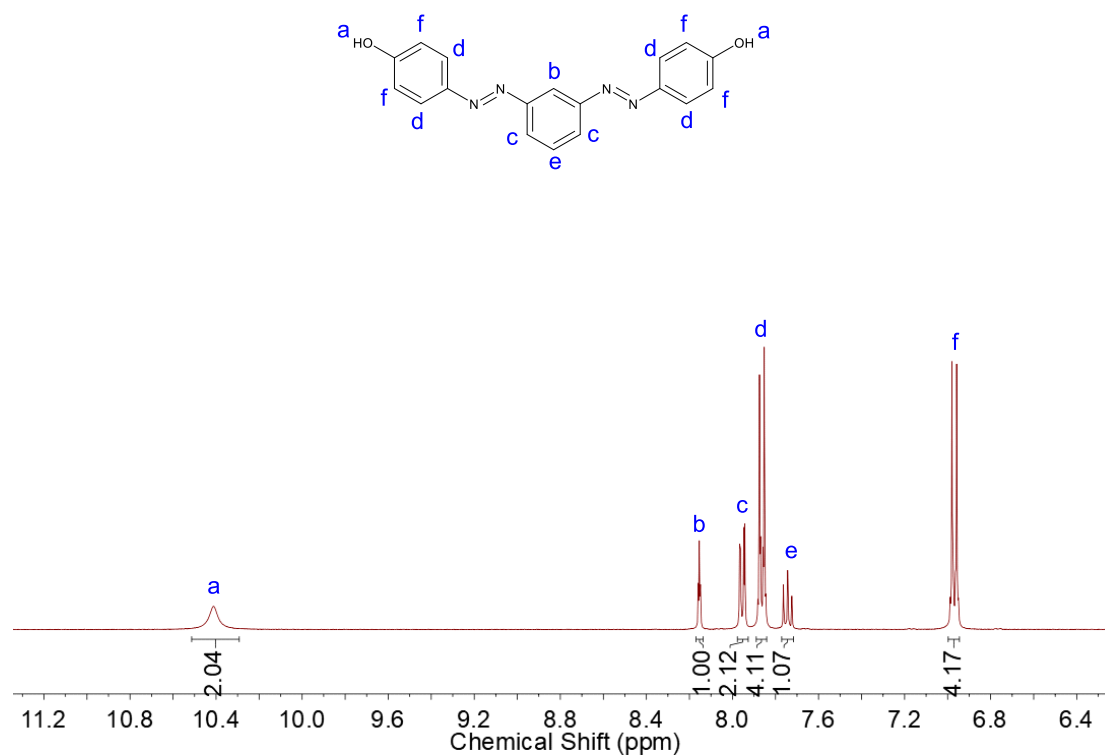
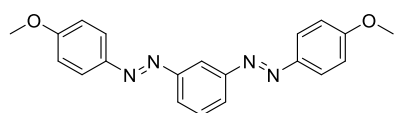


Figure S4. ¹H NMR spectrum of 4,4'-((1*E*,1'*E*)-1,3-phenylenebis(diazene-2,1-diyl))diphenol.



2: To the solution of 4,4'-((1*E*,1'*E*)-1,3-phenylenebis(diazene-2,1-diyl))diphenol (0.68 g, 2.14 mmol, 1.0 equiv) in acetone (40 mL) was added K₂CO₃ (1.48 g, 10.7 mmol, 5.0 equiv) and iodomethane (670 μL, 10.7 mmol, 5.0 equiv). The reaction mixture was refluxed at 40 °C for 15 h. The reaction was monitored by TLC. After completion of

the reaction, the mixture was cooled to room temperature. The mixture was then filtered to remove insolubles such as inorganic salts and the filtrate was concentrated by rotary evaporation. The obtained crude product was purified by recrystallization from methanol to give **2** as a soft yellow cotton-like solid (482.0 mg, 65% yield). ^1H NMR (400 MHz, CDCl_3) δ 8.38 (s, 1 H), 8.00-7.97 (m, 6 H), 7.64 (t, $J = 7.6$ Hz, 1 H), 7.05-7.03 (m, 4 H), 3.91 (s, 6 H).

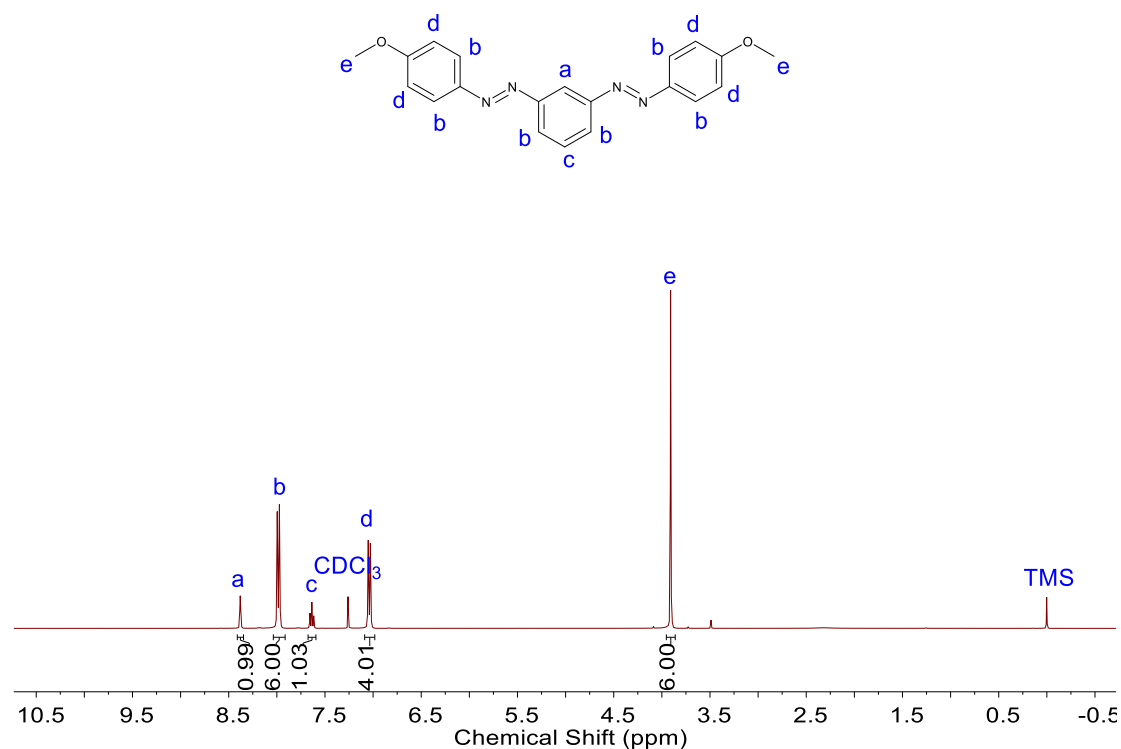


Figure S5. ^1H NMR spectrum of **2**.

4. Synthesis of **3**

The synthesis of **3** was based on the method reported in the literature with minor modifications (Figure S6).^{2,3} The details for the synthesis are provided below.

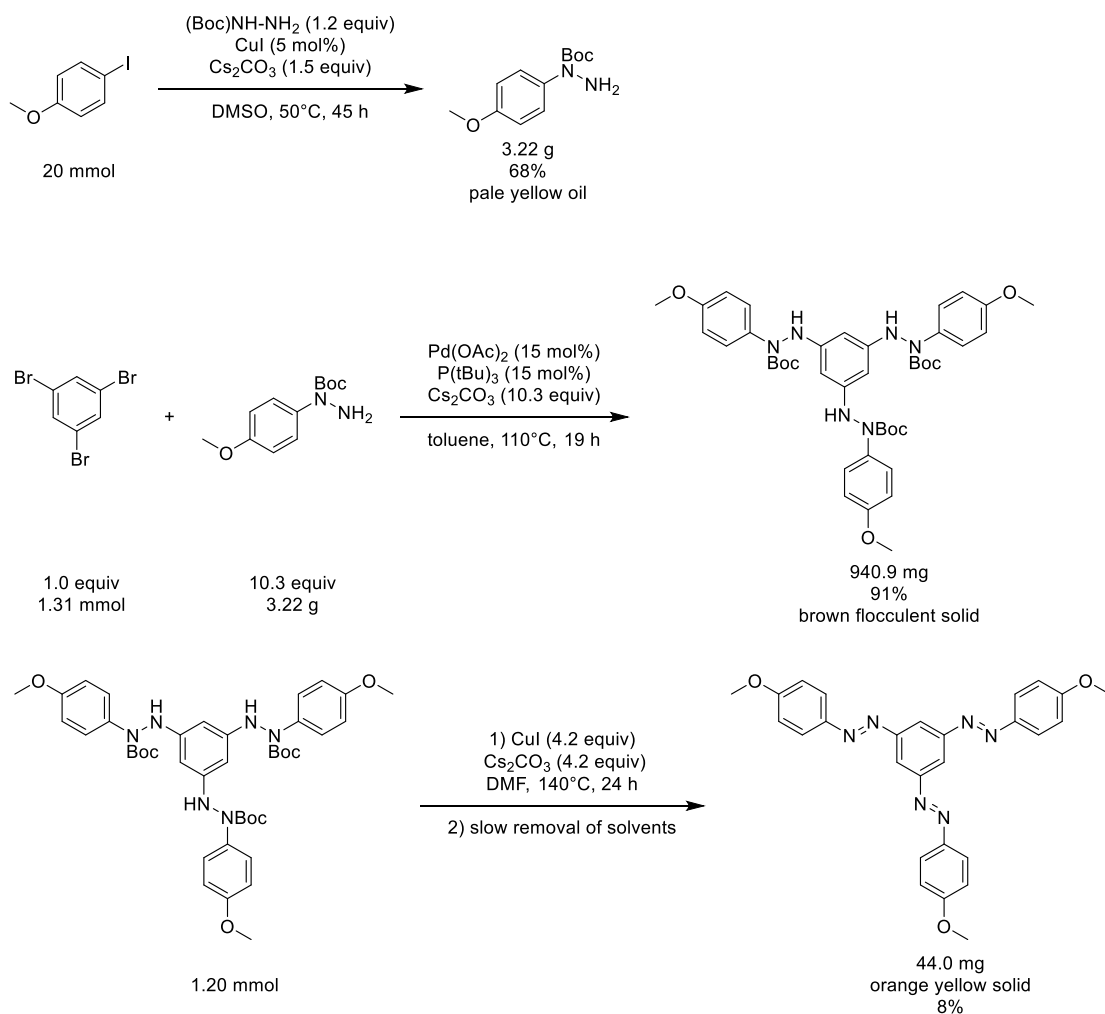
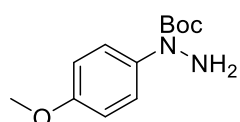


Figure S6. Synthetic route towards **3**.



tert-butyl 1-(4-methoxyphenyl)hydrazine-1-carboxylate: 4-Iodoanisole (4.68 g, 20 mmol, 1.0 equiv), *tert*-butyl carbazate (3.17 g, 24 mmol, 1.2 equiv), CuI (190.5 mg, 1 mmol, 5 mol%), and Cs₂CO₃ (9.77 g, 30 mmol, 1.5 equiv) were weighed directly into a 100 mL round-bottom flask and dried under high vacuum for 30 min. Under nitrogen condition, DMSO (40 mL, extra dry) was added. The mixture was stirred at 50 °C for 45 h. The reaction was monitored by TLC. After completion of the reaction, the mixture was cooled to room temperature. Afterwards, the reaction mixture was diluted with ethyl acetate, filtered through a plug of silica gel (ethyl acetate wash), and the filtrate

was concentrated by rotary evaporation to remove the solvent ethyl acetate. The mixture was diluted with H₂O and the aqueous layer was extracted with ethyl acetate (20 mL×3). The combined organic layers were washed with saturated brines (20 mL×1), dried over Na₂SO₄, filtered, and concentrated by rotary evaporation. The crude product was purified by column chromatography over silica gel (petroleum ether/ethyl acetate/dichloromethane = 15/1/1 - 5/1/1 as the eluent), giving tert-butyl 1-(4-methoxyphenyl)hydrazine-1-carboxylate as pale yellow oil (3.22 g, 68% yield). ¹H NMR (400 MHz, CDCl₃) δ 7.30 (d, *J* = 8.4 Hz, 2 H), 6.84 (d, *J* = 8.4 Hz, 2 H), 4.42 (s, 2 H), 3.80 (s, 3 H), 1.47 (s, 9 H).

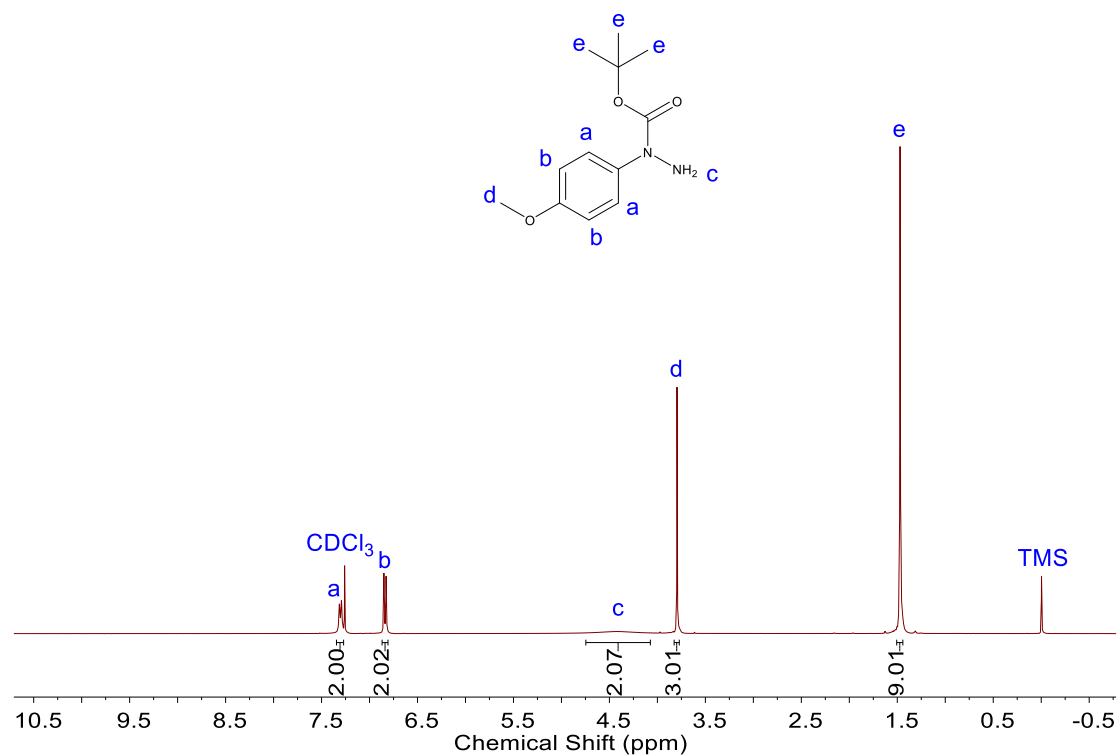
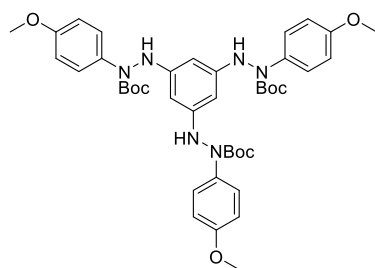


Figure S7. ¹H NMR spectrum of tert-butyl 1-(4-methoxyphenyl)hydrazine-1-carboxylate.



tri-tert-butyl 2,2',2''-(benzene-1,3,5-triyl)tris(1-(4-methoxyphenyl)hydrazine-1-carboxylate): To a flask were charged with Pd(OAc)₂ (44.9 mg, 0.2 mmol, 15 mol%), P(t-Bu)₃ (10% in n-pentane, 650 μL, 0.2 mmol, 15 mol%), and Cs₂CO₃ (4.40 g, 13.51 mmol, 10.3 equiv). Under nitrogen condition, dry toluene (5 mL) was added and the resulting suspension was allowed to stir at ambient temperature for 30 min. To this mixture was added a solution of 1,3,5-tribromobenzene (412.4 mg, 1.31 mmol, 1.0 equiv) and tert-butyl 1-(4-methoxyphenyl)hydrazine-1-carboxylate (3.22 g, 13.51 mmol, 10.3 equiv) in dry toluene (30 mL) via syringe. The reaction mixture was refluxed at 110 °C for 19 h. The reaction was monitored by TLC until 1,3,5-tribromobenzene had been consumed. The mixture was cooled to room temperature, filtered over Celite (ethyl acetate wash), and the filtrate was concentrated by rotary evaporation. The crude product was purified by column chromatography over silica gel (petroleum ether/ethyl acetate/dichloromethane = 10/1/1 - 3/1/1 as the eluent), giving tri-tert-butyl 2,2',2''-(benzene-1,3,5-triyl)tris(1-(4-methoxyphenyl)hydrazine-1-carboxylate) as brown flocculent solid (940.9 mg, 91% yield). ¹H NMR (400 MHz, CDCl₃) δ 7.35 (d, *J* = 8.4 Hz, 6 H), 6.79-6.77 (m, 6 H), 5.84 (s, 3 H), 3.77 (s, 9 H), 1.35 (s, 27 H).

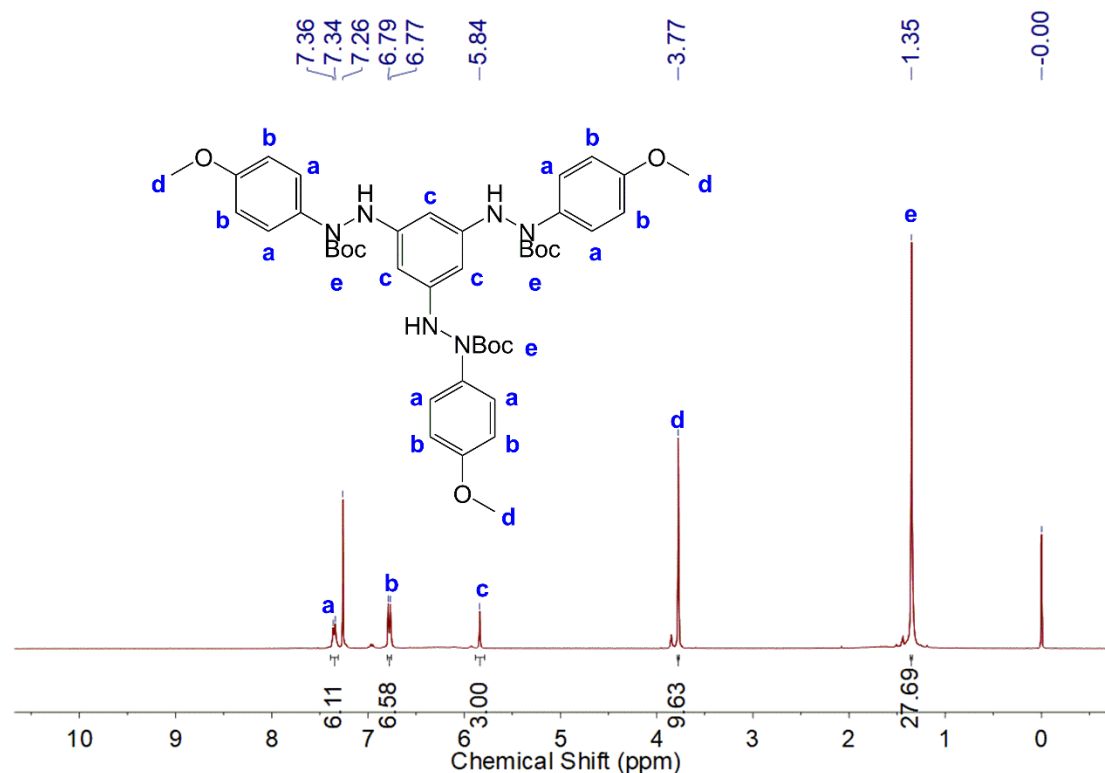
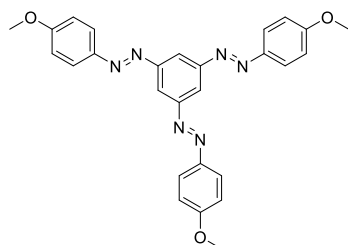


Figure S8. ¹H NMR spectrum of tri-tert-butyl 2,2',2''-(benzene-1,3,5-triyl)tris(1-(4-methoxyphenyl)hydrazine-1-carboxylate).



3: Tri-tert-butyl 2,2',2''-(benzene-1,3,5-triyl)tris(1-(4-methoxyphenyl)hydrazine-1-carboxylate) (940.9 mg, 1.20 mmol, 1.0 equiv), CuI (959.9 mg, 5.04 mmol, 4.2 equiv), and Cs₂CO₃ (1.65 g, 5.04 mmol, 4.2 equiv) were weighed directly into a 100 mL round-bottom flask and dried under high vacuum for 30 min. Under nitrogen condition, dry DMF (18 mL) was added. The mixture was refluxed at 140 °C for 24 h. The reaction was monitored by TLC. After completion of the reaction, the mixture was cooled to room temperature. Afterwards, the reaction mixture was filtered through a plug of silica gel (dichloromethane wash), and the filtrate was concentrated by rotary evaporation. The crude product was purified by column chromatography over silica gel (petroleum ether/ethyl acetate/dichloromethane = 30/1/1 - 10/1/1 as the eluent) to give a mixture

of four isomers of **3**, which were isomerized to the *EEE* isomer (an orange yellow solid, 44.0 mg, 8% yield) upon slow removal of the solvent in the dark. ^1H NMR (400 MHz, CDCl_3) δ 8.48 (s, 3 H), 8.04-8.00 (m, 6 H), 7.07-7.04 (m, 6 H), 3.92 (s, 9 H). ^{13}C NMR (100 MHz, CDCl_3) δ 162.64, 154.21, 147.09, 125.30, 118.02, 114.47, 55.79. HR MS (ESI): Calculated for $\text{C}_{27}\text{H}_{25}\text{O}_3\text{N}_6$ ($\text{M}+\text{H}$) $^+$: 481.19881, found: 481.19788.

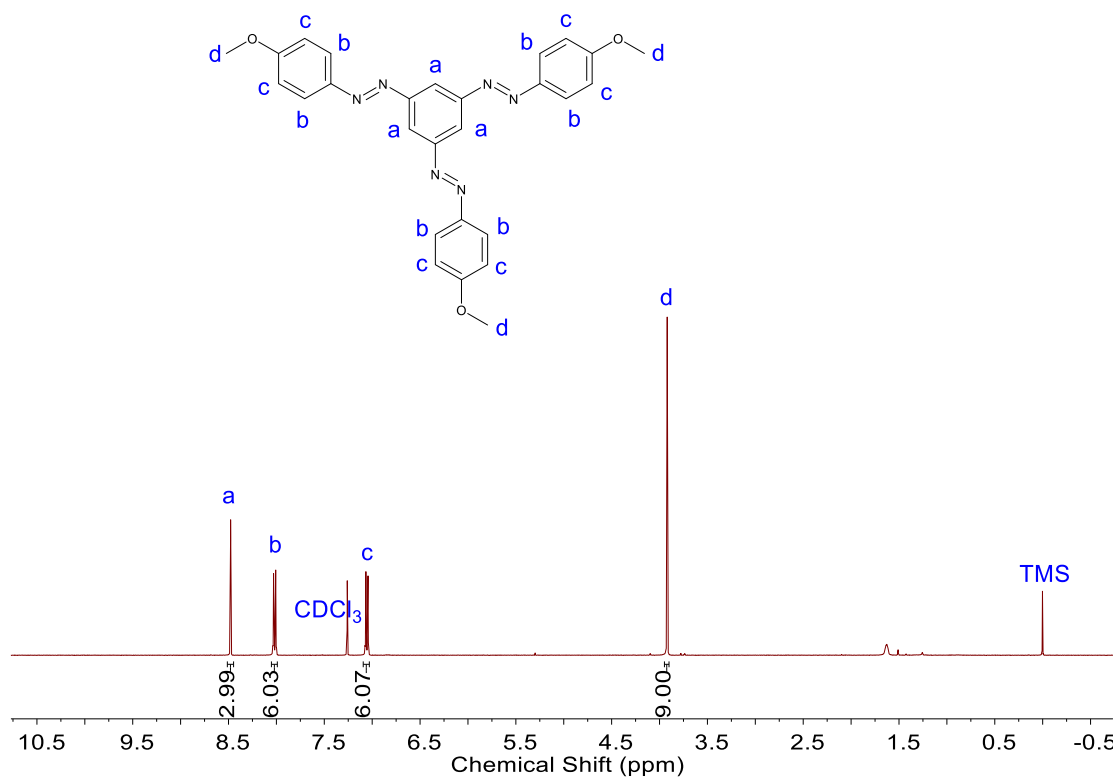


Figure S9. ^1H NMR spectrum of **3**.

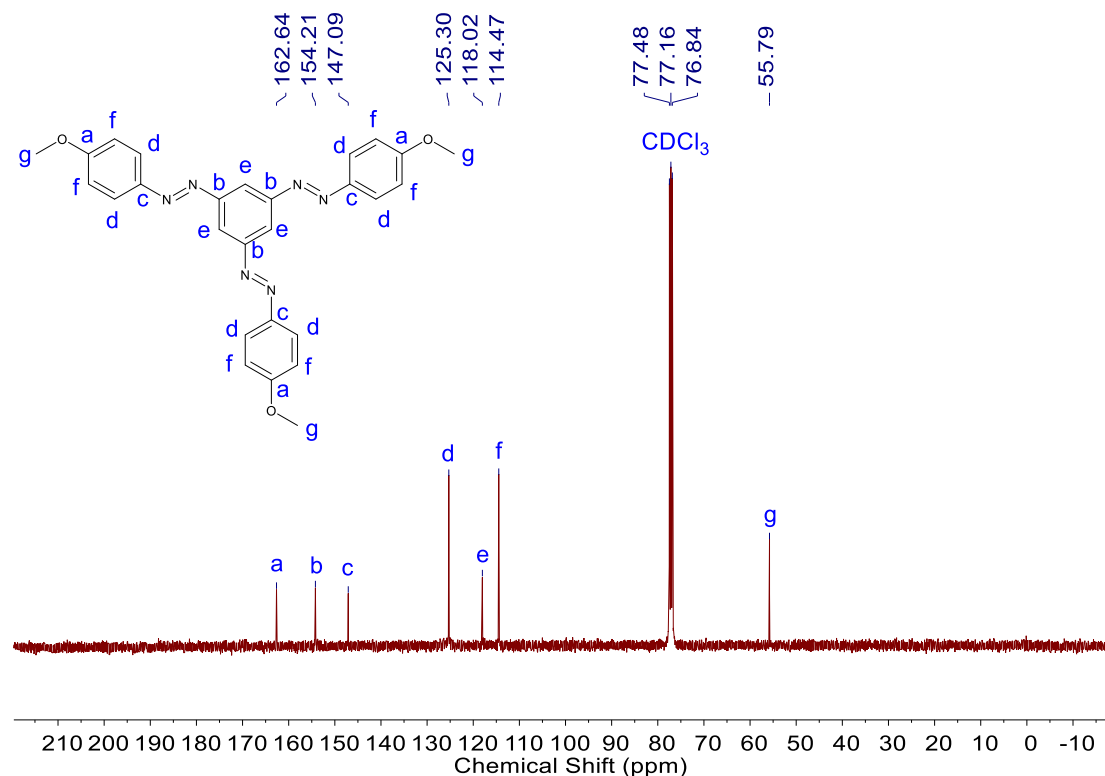


Figure S10. ¹³C NMR spectrum of **3**.

5. Estimation of isomer contents of **1**, **2** and **3**

The isomer contents were estimated by a method reported in literature:^{4,5}

$$Z \text{ content} = (1-A/A_E)/(1-\epsilon_Z/\epsilon_E)$$

$$E \text{ content} = 1-Z \text{ content}$$

where A is the absorbance of photoswitch, A_E is the absorbance of E photoswitch, and ϵ_Z and ϵ_E are the molar absorption coefficients of Z and E isomers, respectively, at the wavelength of maximum absorption. ϵ_Z/ϵ_E for azobenzene is close to 0.05.^{4,5} Note: the estimated isomer content is an average number.

6. Quantum yield measurements for E -to- Z photoisomerization in solution

Photoisomerization quantum yield (ϕ) was measured using an established method in

literature.⁶ Tetrahydrofuran (THF) solutions of the azo compounds with the absorbance of ~ 1.5 of the $\pi\text{-}\pi^*$ transition band were prepared for the measurement. The $\pi\text{-}\pi^*$ transition bands are at 347 nm, 357 nm, and 361 nm for compounds **1**, **2**, and **3**, respectively.

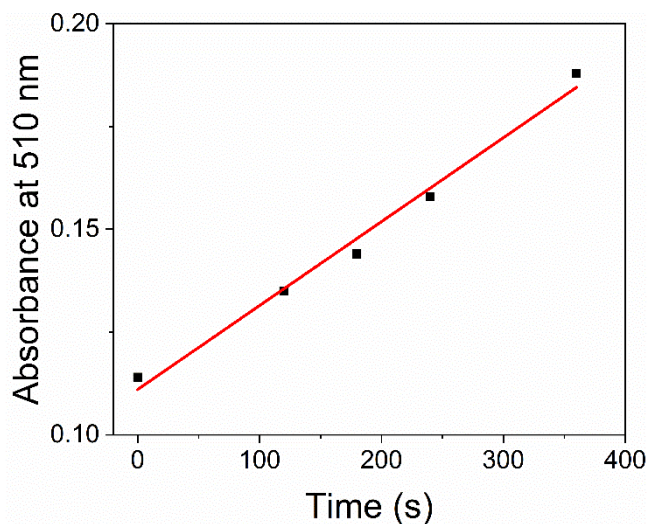


Figure S11. Absorbance of the tris-phenanthroline iron (II) complex as a function of irradiation time of potassium ferrioxalate (black squares). The red line shows a linear fit, giving the photon flux for 365 nm LED as $1.52 \times 10^{-9} \text{ mol s}^{-1}$.

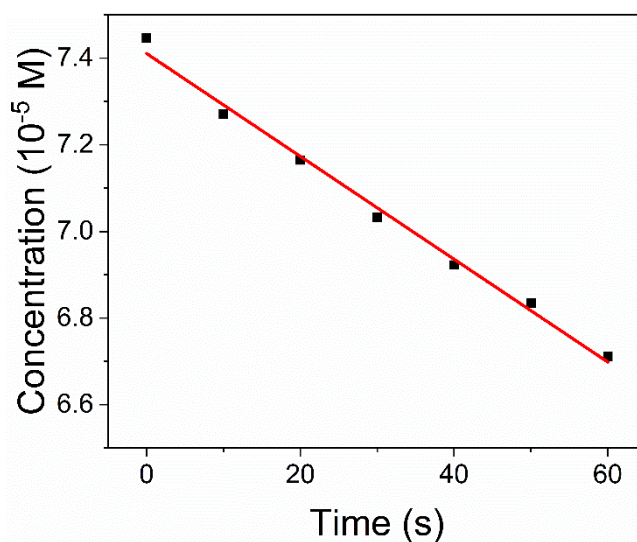


Figure S12. Quantum yield measurements for **1** under the irradiation of 365 nm light. The red line shows a linear fit. $\phi_1 = 23\%$.

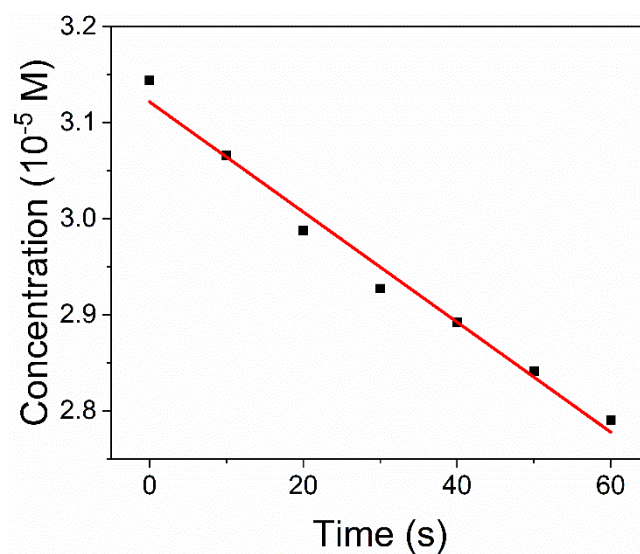


Figure S13. Quantum yield measurements for **2** under the irradiation of 365 nm light. The red line shows a linear fit. $\phi_2 = 11\%$.

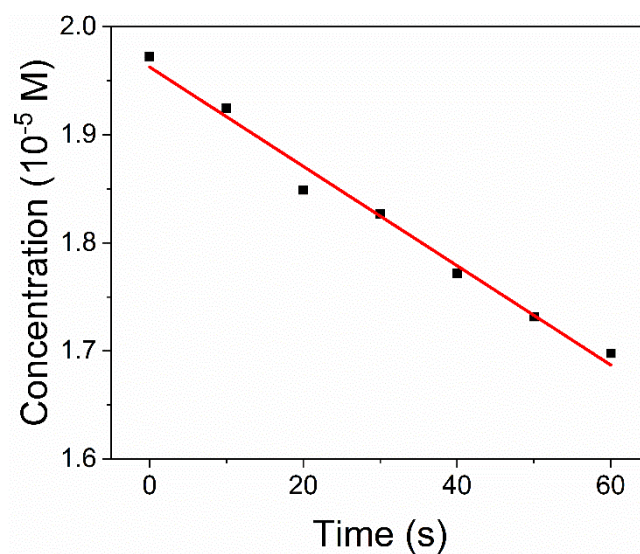


Figure S14. Quantum yield measurements for **3** under the irradiation of 365 nm light. The red line shows a linear fit. $\phi_3 = 9\%$.

7. The first-order rate constant (k) and half-life ($\tau_{1/2}$) values for *Z*-to-*E* reversion

The first-order rate constants (k) and half-lives ($\tau_{1/2}$) for *Z*-to-*E* reversion were measured by a method reported in literature:⁷⁻⁹

$$\ln\left(\frac{A_\infty - A_t}{A_\infty - A_0}\right) = -kt$$

$$\tau_{1/2} = \frac{\ln 2}{k}$$

where A_∞ is the absorption of azobenzenes in thermally stable E state, A_t is the absorption of azobenzenes kept in the dark for a time t , and A_0 is the absorption of azobenzenes at the metastable Z state after UV irradiation.

8. Procedures for charging in solutions

The procedures for charging in solutions were based on the method reported in our previous work with minor modifications.⁵ In brief, the **1- E** , **2- EE** , or **3- EEE** (30 mg) was dissolved in DCM (2.5 mL). The solution was irradiated with 365 nm light (4.5 mW/cm²) for 3 h under stirring to induce an E -to- Z isomerization until UV-vis absorption spectra showed that the samples had reached their photostationary state (PSS). DCM was removed using a rotary evaporator at 10–25 mbar for 5 min and a vacuum pump at ambient temperature for 10 min. The dried Z sample was quickly transferred to a DSC sample pan, and the measurements were taken immediately. Meanwhile, the residual sample was dissolved in CDCl₃ to measure the Z content using ¹H NMR spectroscopy.

9. Procedures for charging in solid states

9.1 Experimental setup for charging in solid states

We made an experimental setup for charging in solid states via UV light irradiation (Figure S11). We cut the bottom of a commercially available 5 mL glass test tube with a glass cutter to a length of 3 cm and used it as a “reaction flask” for charging via UV light irradiation. Then, we glued the “reaction flask” to a small vial cap to fix it so that the device could be firmly fixed to the magnetic stirrer with a layer of double-sided tape

on the surface to prevent the “reaction flask” from shaking during stirring. Finally, a UV LED (365 nm) was fixed at 5 cm above the “reaction flask”. Thus, the experimental setup for charging in solid states was accomplished, which could realize irradiation and stirring at the same time.

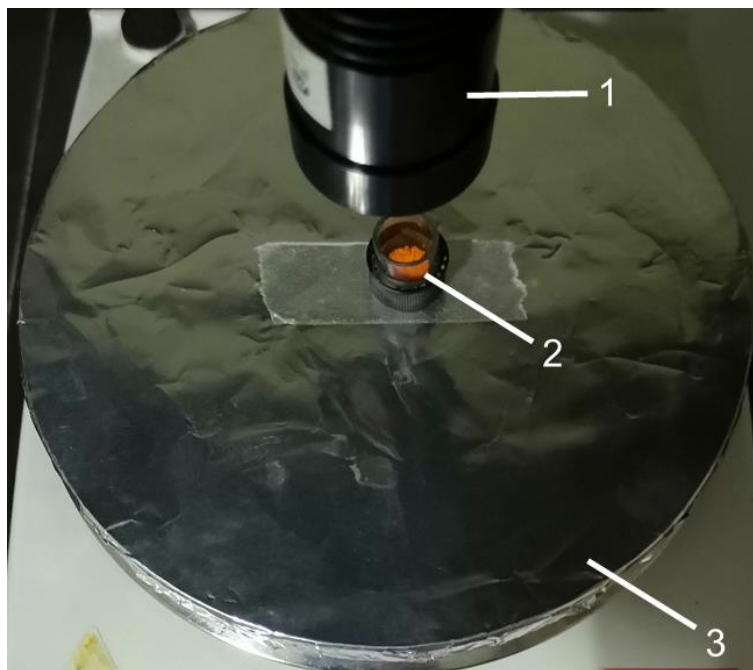


Figure S15. Experimental setup for charging in solid states via UV light irradiation. 1—UV LED; 2—homemade glass “reaction flask”; 3—magnetic stirrer.

9.2 Procedures for charging

We weighed the solid powders (20 mg) into a homemade “reaction flask”, and turned on the UV LED (365 nm, 220.3 mW/cm²) for photocharging. Subsequently, we added a rice-grain-sized magnet to the “reaction flask”, and turned on the magnetic stirrer. Finally, the sample was in a state of being irradiated and stirred simultaneously, and the whole was relatively uniform. After charging for 12 h, the sample was quickly transferred to a DSC sample pan, and the measurements were taken immediately. Meanwhile, the residual sample was dissolved in CDCl₃ to measure the Z content using ¹H NMR spectroscopy.

10. TGA curves of 1, 2 and 3

We tested the thermal stability of **1**, **2** and **3** by thermogravimetric analysis (TGA) (Figure S12). The decomposition temperature T_d (5 wt%) was defined as 5% weight loss temperature. The T_d (5 wt%) value of **1** was 173 °C, and only one step of degradation occurred in the test temperature range (Figure S12, black curve). The T_d (5 wt%) value of **2** was 287 °C, and only one step of degradation occurred in the test temperature range (Figure S12, red curve), indicating that the two azobenzene groups in **2** decomposed simultaneously. The T_d (5 wt%) value of **3** was 360 °C, and the degradation occurred in two steps in the test temperature range (Figure S12, blue curve). From the analysis of the change in mass fraction of **3**, firstly, one azobenzene group was decomposed below 390 °C, and the remaining two azobenzene groups were decomposed simultaneously above 390 °C. The T_d (5 wt%) values of **1**, **2** and **3** showed that the thermal stability of azobenzene derivative molecules increased gradually with the increase in the number of azobenzene groups.

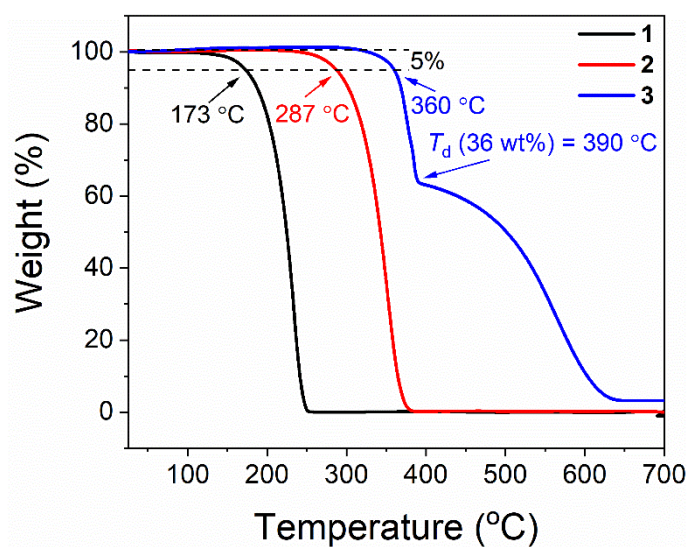


Figure S16. TGA curves of **1**, **2** and **3**.

11. DSC curves for 1-*E*, 2-*EE*, and 3-*EEE*

We conducted DSC tests on **1-*E***, **2-*EE***, and **3-*EEE***, respectively (Figure S13). The high temperature range was selected to be lower than the respective T_d (5 wt%) to prevent

the samples from decomposing during the tests. **1-E** had a sharp endothermic peak at 56.97 °C during the heating process, which corresponded to the melting of a solid crystal into an isotropic phase (Figure S13a, red curve). In the subsequent cooling process, **1-E** exhibited a sharp exothermic peak at 31.15 °C and the sample began to crystallize, transforming from an isotropic phase to a solid crystal (Figure S13a, black curve). In contrast, **2-EE** had a melting point of 112.68 °C and a crystallization point of 82.33 °C; **3-EEE** had a melting point of 179.94 °C and a crystallization point of 132.94 °C. The DSC results of **1-E**, **2-EE**, and **3-EEE** showed that the melting points of azobenzene derivative molecules increased gradually with the increase in the number of azobenzene groups.

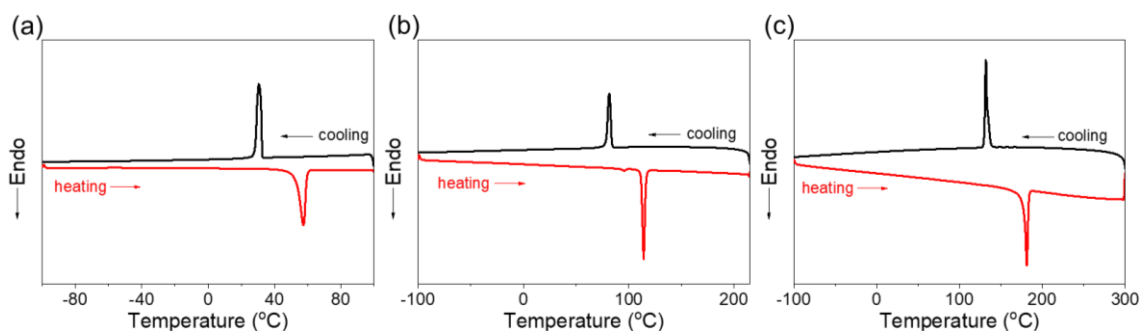


Figure S17. DSC curves of (a) **1-E**, (b) **2-EE** and (c) **3-EEE**.

12. Energy storage performances when charged in solution under a solar lamp

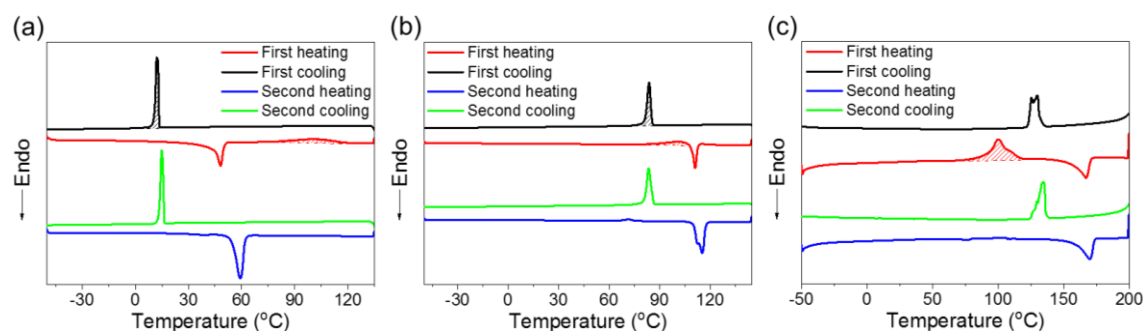


Figure S18. DSC curves of (a) **1**, (b) **2** and (c) **3** which were charged in DCM solutions via solar lamp irradiation. The DSC measurements were performed at 10 °C/min under a N₂ atmosphere.

Table S1. The energy densities for **1**, **2** and **3** charged in DCM solutions via solar lamp irradiation.

Compound	1	2	3
ΔH_{iso} (J/g)	25 ± 0.3	8 ± 0.1	-
ΔH_{cry} (J/g)	51 ± 0.5	62 ± 0.6	-
ΔH_{total} (J/g)	76 ± 0.8	70 ± 0.7	78 ± 0.8

13. XRD patterns of **1**

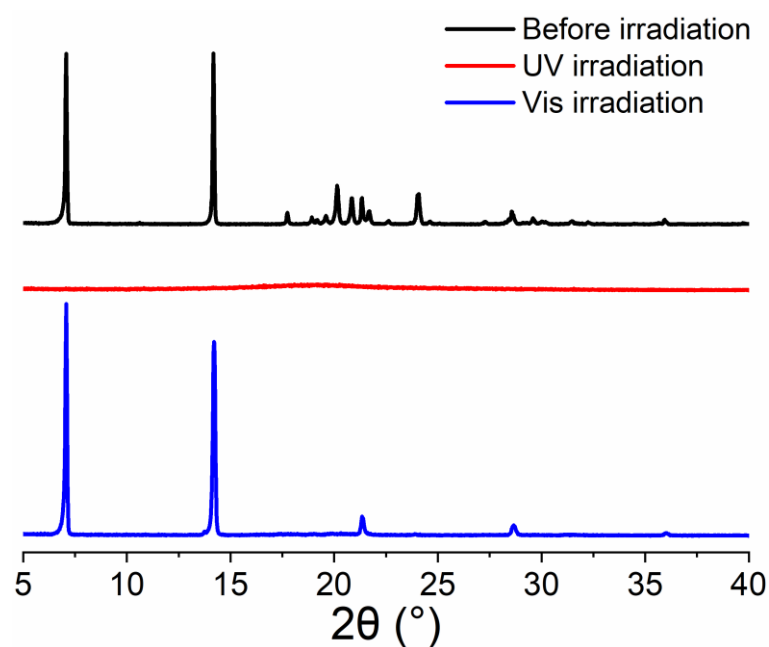
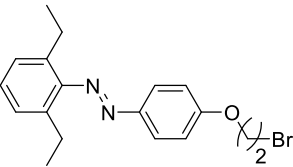
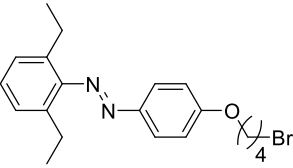
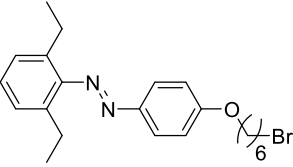
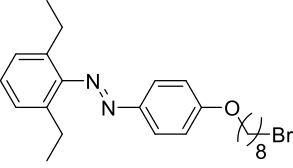
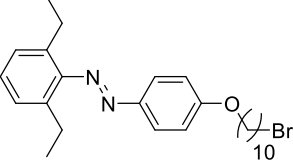
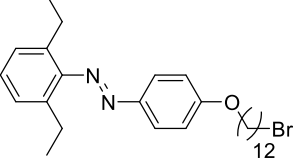
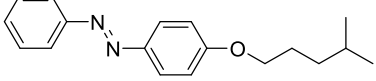
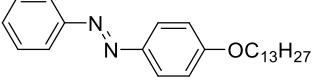
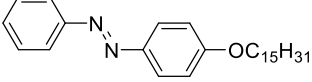


Figure S19. XRD patterns of **1** before irradiation, after UV light irradiation (365 nm, 220.3 mW/cm²) for 30 min, and after subsequent visible light irradiation (530 nm, 101.7 mW/cm²) for 30 min.

14. The energy densities of some liquid and photoliquefiable azobenzene derivatives reported in literature

Table S2. A list of energy densities of some liquid and photoliquefiable azobenzene derivatives reported in literature.

Molecular structure	ΔH_{total} (J/g)	Reference
	104.06	10
	96.65	10
	80.25	10
	145.95	10
	118.56	10
	91.78	10
	181	11
	170.5	12
	198.4	12

15. Energy storage performances when charged in solid state under simulated sunlight irradiation

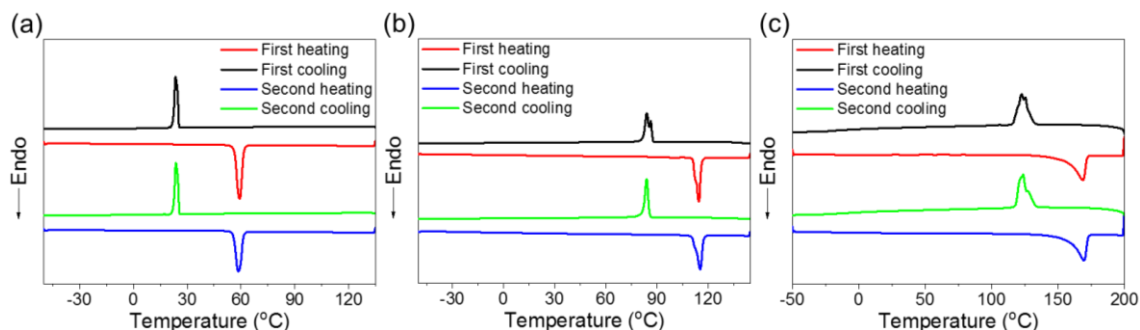


Figure S20. DSC curves of (a) **1**, (b) **2** and (c) **3** charged in solid states via solar lamp irradiation.

The DSC measurements were performed at 10 °C/min under a N₂ atmosphere.

Table S3. The energy densities of **1**, **2** and **3** charged in solid states via sunlamp irradiation.

Compound	1	2	3
ΔH_{iso} (J/g)	0	0	0
ΔH_{cry} (J/g)	0	0	0
ΔH_{total} (J/g)	0	0	0

16. Energy conversion efficiency (ECE) calculation

Energy conversion efficiency (ECE) can be defined as:

$$\eta = \frac{E_{\text{output}}}{E_{\text{input}}}$$

where E_{input} is the total energy input, and E_{output} is the total energy output of the storage system.¹³

Here, we used a simplified method to calculate the E_{input} and E_{output} :¹⁴

$$E_{\text{input}} = I \times S \times t$$

$$E_{output} = \Delta H_{total} \times m$$

where I is the light intensity of a UV LED used for charging, S is the irradiation area, t is the irradiation time, ΔH_{total} is the total energy density, and m is the mass of the sample used for charging.

Table S4. Energy conversion efficiency for **1**, **2** and **3** charged in DCM solutions via UV light irradiation.

Compound	1	2	3
E_{input} (J)	194.40	194.40	194.40
E_{output} (J)	7.65	8.16	7.26
η (%)	3.9	4.2	3.7

Table S5. Energy conversion efficiency for **1**, **2** and **3** charged in solid states via UV light irradiation.

Compound	1	2	3
E_{input} (J)	11516	11516	11516
E_{output} (J)	4.74	0	0
η (%)	0.04	0	0

17. Supplementary movies

Movie S1. Charging of **1** in solvent-free state via UV light irradiation under magnetic stirring.

Movie S2. Charging of **2** in solvent-free state via UV light irradiation under magnetic stirring.

Movie S3. Charging of **3** in solvent-free state via UV light irradiation under magnetic stirring.

18. References

1. F. Cisnetti, R. Ballardini, A. Credi, M. T. Gandolfi, S. Masiero, F. Negri, S. Pieraccini and G. P. Spada, *Chem. – Eur. J.*, 2004, **10**, 2011-2021.
2. A. H. Heindl and H. A. Wegner, *Beilstein J. Org. Chem.*, 2020, **16**, 22-31.
3. Y.-K. Lim, S. Choi, K. B. Park and C.-G. Cho, *J. Org. Chem.*, 2004, **69**, 2603-2606.
4. J. G. Victor and J. M. Torkelson, *Macromolecules*, 1987, **20**, 2241-2250.
5. H. Zhou, C. Xue, P. Weis, Y. Suzuki, S. Huang, K. Koynov, G. K. Auernhammer, R. Berger, H.-J. Butt and S. Wu, *Nat. Chem.*, 2017, **9**, 145-151.
6. K. Stranius and K. Börjesson, *Sci. Rep.*, 2017, **7**, 41145.
7. M.-a. Morikawa, Y. Yamanaka and N. Kimizuka, *Chem. Lett.*, 2022, **51**, 402-406.
8. L. Dong, Y. Chen, F. Zhai, L. Tang, W. Gao, J. Tang, Y. Feng and W. Feng, *J. Mater. Chem. A*, 2020, **8**, 18668-18676.
9. S. Smith and F. Bou-Abdallah, *J. Thermodyn. Catal.*, 2017, **8**, 1-6.
10. Y. Yang, S. Huang, Y. Ma, J. Yi, Y. Jiang, X. Chang and Q. Li, *ACS Appl. Mater. Interfaces*, 2022, **14**, 35623-35634.
11. J. Tang, Y. Feng and W. Feng, *Compos. Commun.*, 2021, **23**, 100575.
12. H. Liu, Y. Feng and W. Feng, *Compos. Commun.*, 2020, **21**, 100402.
13. Y. Shi, M. A. Gerkman, Q. Qiu, S. Zhang and G. G. D. Han, *J. Mater. Chem. A*, 2021, **9**, 9798-9808.
14. R. Zhao, Y. Li, J. Bai, J. Mu, L. Chen, N. Zhang, J. Han, F. Liu and S. Yan, *Dyes and Pigments*, 2022, **202**, 110277.